

# Nonprobabilistic Interval Reliability Analysis of Wing Flutter

Xiaojun Wang\* and Zhiping Qiu†

*Beijing University of Aeronautics and Astronautics, 100191 Beijing, People's Republic of China*

DOI: 10.2514/1.39880

The influences of uncertainties on the flutter behavior of aeroelastic wings were investigated. Uncertainties in the structural parameters of the wing and the natural wind speed were quantified by interval numbers. Uncertainty propagation in wing flutter was studied via interval analysis, and the interval estimation of flutter wind speed of the wing was obtained. Further, the reliability of wing flutter was analyzed based on the interval flutter-wind-speed and natural-wind-speed interference model. The ratio of the volume of the safe region to the total volume of the region associated with the variation of the basic interval variables is suggested as the measure of structural nonprobabilistic reliability. Numerical examples were used to illustrate the validity of the presented measurement.

## I. Introduction

**A**EROYNAMIC instability takes place when an aeroelastic structure is exposed to wind speed above a certain critical value that can be predicted by wind-tunnel tests or theoretical calculation with experimentally obtained parameters. The flutter speed is an important assessment index for the dynamic stability of aeroelastic structures [1]. However, because most of these parameters involved in the prediction are physically uncertain variables and/or subjectively assumed values because of a lack of complete knowledge, it would make more sense to carry out a reliability analysis to determine the possibility of the aeroelastic structure failure due to flutter than to state a single critical wind speed [2].

Up to now, the assessments of critical conditions for flutter of aeroelastic structures were mainly performed in a probabilistic framework. Ito and Fujino [3] made a probabilistic study of torsional flutter for the proposed Akashi Strait Bridge, in which a stochastic model of the critical flutter speed was adopted with a deterministic concept of the maximum wind speed at the site. In the case of the Great Belt Bridge, Ostenfeld-Rosenthal et al. [4] demonstrated the presentation of an aerodynamic instability criterion by describing both resistance and load variables using stochastic models. Ge and Xiang [5] studied the random influences of self-excited aerodynamic force or aerodynamic derivatives and established the stochastic finite element model for the flutter analysis of the bridge; based on this model, the reliability problem of bridge flutter with random factors was studied [6,7]. Liu et al. [8] considered the randomness in the structural stiffness and mass distribution of the wing and studied the probabilistic reliability analysis of wing flutter. All of these applications of reliability models have significantly helped to understand the account of uncertainties in the structures and loads and have led to a clear failure probability due to flutter.

However, in fact, the test samples of structures are usually scant, so that the statistical data are difficult to obtain, whereas the bounds of uncertain information are easier to determine [9,10]. Thus, the set-based theoretical convex methods have emerged, including convex models [11] and interval analysis [12–14], which describe the uncertain parameters by the bounded convex set.

In this paper, the influences of uncertainties on the wing flutter are investigated. By describing the uncertain factors with the interval numbers, the influences of them on flutter speed of the wing are analyzed by the interval finite element model, which gives the

approximately estimated interval of flutter speed. By combining with the nonprobabilistic interval reliability theory presented in [15], the nonprobabilistic reliability analysis of wing flutter is performed.

## II. Deterministic Flutter Analysis of the Wing

A flutter analysis determines the dynamic stability of an aeroelastic system. Three methods of analysis are available: the American (K) method, a restricted but more efficient American (KE) method, and the British (PK) method. The PK method produces results only at the velocities of interest to the analyst. The PK method treats the aerodynamic matrices as real frequency-dependent springs and dampers. A frequency is estimated, and the eigenvalues are found. From an eigenvalue, a new frequency is found. The convergence to a consistent root is rapid. Advantages of the method are that it permits control systems analysis and that the damping values obtained at subcritical flutter conditions appear to be more representative of the physical damping. Another advantage occurs when the stability at a specified velocity is required, because many fewer eigenvalue analyses are needed to find the behavior at one velocity. The input data for the PK method also allows looping. The inner loop of the user data is on velocity, with Mach number and density on the outer loops. Thus, finding the effects of variations in one or both of the two parameters in one run is possible. For the sake of convenience with the following formulation, the concise procedure for the PK method (for details, see [5]) is given in this section. According to the condition of dynamic equilibrium of the wing, the finite element flutter equation can be expressed as

$$\mathbf{M} \ddot{\boldsymbol{\delta}}(t) + \mathbf{D} \dot{\boldsymbol{\delta}}(t) + \mathbf{K} \boldsymbol{\delta}(t) = \mathbf{A}(t) \quad (1)$$

where  $\mathbf{M}$ ,  $\mathbf{D}$ , and  $\mathbf{K}$  are, respectively, the global mass matrix, the global damping matrix, and the global stiffness matrix of the wing;  $\mathbf{A}(t)$  is the global aerodynamic force vector; and

$$\mathbf{A}(t) = \frac{1}{2} \rho U^2 \left( \mathbf{A}_s \boldsymbol{\delta}(t) + \frac{1}{U} \mathbf{A}_d \dot{\boldsymbol{\delta}}(t) \right) \quad (2)$$

where  $\mathbf{A}_s$  and  $\mathbf{A}_d$  are, respectively, the global aerodynamic stiffness matrix and the global aerodynamic damping matrix;  $U$  and  $\rho$  are, respectively, the horizontal freestream velocity and the air density; and  $\boldsymbol{\delta}(t)$  is the global nodal displacement vector of the wing, in virtue of modal decomposition method, which can be expressed as

$$\boldsymbol{\delta}(t) = \boldsymbol{\Phi} \boldsymbol{\xi}(t) \quad (3)$$

where  $\boldsymbol{\Phi}$  is the modal matrix and  $\boldsymbol{\xi}(t)$  is the modal coordinate vector.

By substituting Eqs. (2) and (3) into Eq. (1) and premultiplying the transposed modal matrix  $\boldsymbol{\Phi}^T$ , we can obtain

$$\mathbf{M}^g \ddot{\boldsymbol{\xi}} + \mathbf{D}^g \dot{\boldsymbol{\xi}} + \mathbf{K}^g \boldsymbol{\xi} = \frac{1}{2} \rho U^2 \left( \mathbf{A}_s^g \boldsymbol{\xi} + \frac{1}{U} \mathbf{A}_d^g \dot{\boldsymbol{\xi}} \right) \quad (4)$$

Received 19 July 2008; revision received 5 December 2008; accepted for publication 8 December 2008. Copyright © 2008 by the American Institute of Aeronautics and Astronautics, Inc. All rights reserved. Copies of this paper may be made for personal or internal use, on condition that the copier pay the \$10.00 per-copy fee to the Copyright Clearance Center, Inc., 222 Rosewood Drive, Danvers, MA 01923; include the code 0001-1452/09 \$10.00 in correspondence with the CCC.

\*Institute of Solid Mechanics; XJWang@buaa.edu.cn.

†Institute of Solid Mechanics; ZPQiu@buaa.edu.cn.

which is called the modal flutter equation, where  $\mathbf{M}^g = \Phi^T \mathbf{M} \Phi$  is the modal mass matrix,  $\mathbf{D}^g = \Phi^T \mathbf{D} \Phi$  is the modal damping matrix,  $\mathbf{K}^g = \Phi^T \mathbf{K} \Phi$  is the modal stiffness matrix,  $\mathbf{A}_s^g = \Phi^T \mathbf{A}_s \Phi$  is the modal aerodynamic stiffness matrix, and  $\mathbf{A}_d^g = \Phi^T \mathbf{A}_d \Phi$  is the modal aerodynamic damping matrix.

The wing will sustain the harmonic motion at the time of flutter. The modal coordinate is assumed to be of the following form:

$$\xi = \xi_0 \exp(\lambda t) \quad (5)$$

where  $\xi_0$  and  $\lambda$  represent, respectively, the amplitude vector and complex eigenvalue of flutter response, and

$$\lambda = (\Delta + i)\omega \quad (6)$$

where  $\Delta$  is the transient decay rate coefficient,  $\omega$  is the circular frequency, and

$$\omega = kU/B \quad (7)$$

So the reduced frequency is  $k = B\omega/U$ , where  $B$  is half of the reference length. Substituting Eqs. (6) and (7) into Eq. (5) yields

$$\xi = \xi_0 \exp\left(\frac{U}{B}k(\Delta + i)t\right) \quad (8)$$

Substituting Eq. (8) into Eq. (4), we can obtain

$$\begin{aligned} & \left( \mathbf{M}^g \left( \frac{U}{B} \right)^2 k^2 (\Delta + i)^2 + \mathbf{D}^g \left( \frac{U}{B} \right) k (\Delta + i) \right. \\ & \left. + \mathbf{K}^g - \frac{1}{2} \rho U^2 \left( \mathbf{A}_s^g + \frac{k}{B} \mathbf{A}_d^g (\Delta + i) \right) \right) \xi_0 \exp\left(\frac{U}{B}k(\Delta + i)t\right) = 0 \end{aligned} \quad (9)$$

The flutter of the wing corresponds to the constant amplitude motion with zero damping: namely,  $\Delta = 0$  or  $k(\Delta + i) = ki$ . Because of

$$\xi_0 \exp(Uk(\Delta + i)t/B) \neq 0$$

the determinant of coefficient matrix should be zero. The flutter equation of the PK method can be obtained as

$$\begin{aligned} & \left| \mathbf{M}^g \left( \frac{U}{B} \right)^2 k^2 (\Delta + i)^2 + \mathbf{D}^g \left( \frac{U}{B} \right) k (\Delta + i) \right. \\ & \left. + \mathbf{K}^g - \frac{1}{2} \rho U^2 \left( \mathbf{A}_s^g + \frac{ik}{B} \mathbf{A}_d^g \right) \right| = 0 \end{aligned} \quad (10)$$

### III. Interval Finite Element Analysis of Wing Flutter

The flutter equation for the PK method includes the structural parameters such as mass, damping, stiffness, etc., which can be represented as

$$\mathbf{a} = (a_1, a_2, \dots, a_m)^T \quad (11)$$

In the deterministic flutter analysis of the wing, only the deterministic value or nominal value  $\mathbf{a}_0$  of these structural parameters is considered. However, in the uncertain flutter analysis of the wing, the influence of the uncertainty of structural parameters on the wing stability also needs to be considered.

In practice, no sufficient information on uncertainty can usually be obtained, and so it is difficult to determine their statistical characteristics. Nevertheless, the bounds of uncertain parameters can often be defined easily. They can be described by interval notation as

$$\mathbf{a} \in \mathbf{a}^I = [\underline{\mathbf{a}}, \bar{\mathbf{a}}] = [\mathbf{a}_0 - \Delta \mathbf{a}, \mathbf{a}_0 + \Delta \mathbf{a}] = (a_i^I) \quad (12)$$

or

$$a_i \in a_i^I = [\underline{a}_i, \bar{a}_i] = [a_{0i} - \Delta a_i, a_{0i} + \Delta a_i], \quad i = 1, 2, \dots, m \quad (13)$$

where  $\bar{\mathbf{a}} = (\bar{a}_i)$  and  $\underline{\mathbf{a}} = (\underline{a}_i)$  are, respectively, the upper bound and lower bound of structural parameter vector  $\mathbf{a} = (a_i)$ .

The structural parameter vector is slightly different from the nominal value  $\mathbf{a}_0$  and can be denoted by

$$\mathbf{a} = \mathbf{a}_0 + \delta \mathbf{a} \quad \text{or} \quad a_i = a_{0i} + \delta a_i, \quad i = 1, 2, \dots, m \quad (14)$$

where  $\delta \mathbf{a} = (\delta a_i) \in R^m$  is a small uncertain quantity. By comparing Eqs. (12–14), it can be found that the following expression holds:

$$|\delta \mathbf{a}| \leq \Delta \mathbf{a} \quad \text{or} \quad |\delta a_i| \leq \Delta a_i \quad (15)$$

Therefore, the problem of flutter analysis of the wing with uncertainty can be stated as solving the varying ranges of circular frequency  $\omega$  and transient decay rate coefficient  $\Delta$  in complex eigenvalue  $\lambda$  under the constraint Eq. (15) and then obtaining the varying range of flutter speed  $U_{cr}$ . However, it is very difficult to obtain the exact interval of flutter speed. Thus, it is expected that an approximately estimated interval of  $U_{cr}$  can be given.

With the help of first-order Taylor series expansion, the circular frequency  $\omega$  and transient decay rate coefficient  $\Delta$  in complex eigenvalue  $\lambda$  can be approximately expressed as

$$\omega(\mathbf{a}, U) = \omega(\mathbf{a}_0, U) + \sum_{i=1}^m \frac{\partial \omega(\mathbf{a}_0, U)}{\partial a_i} \delta a_i \quad (16)$$

and

$$\Delta(\mathbf{a}, U) = \Delta(\mathbf{a}_0, U) + \sum_{i=1}^m \frac{\partial \Delta(\mathbf{a}_0, U)}{\partial a_i} \delta a_i \quad (17)$$

By applying the natural interval extension [12,13] (which is to replace the real variables in the real-value function by the corresponding interval variables to obtain the interval-value function and to replace the arithmetic operations by the corresponding interval arithmetic) to Eqs. (16) and (17), the intervals of  $\omega$  and  $\Delta$  can be obtained, respectively, as

$$\omega^I(\mathbf{a}, U) = \omega(\mathbf{a}_0, U) + \sum_{i=1}^m \left| \frac{\partial \omega(\mathbf{a}_0, U)}{\partial a_i} \right| \Delta a_i^I \quad (18)$$

and

$$\Delta^I(\mathbf{a}, U) = \Delta(\mathbf{a}_0, U) + \sum_{i=1}^m \left| \frac{\partial \Delta(\mathbf{a}_0, U)}{\partial a_i} \right| \Delta a_i^I \quad (19)$$

After the interval operations, and according to the necessary and sufficient condition of the equality of interval numbers, the lower-bound curve and upper-bound curve of circular frequency  $\omega$  varying with  $U$  are, respectively,

$$\underline{\omega}(\mathbf{a}, U) = \omega(\mathbf{a}_0, U) - \sum_{i=1}^m \left| \frac{\partial \omega(\mathbf{a}_0, U)}{\partial a_i} \right| \Delta a_i \quad (20)$$

and

$$\bar{\omega}(\mathbf{a}, U) = \omega(\mathbf{a}_0, U) + \sum_{i=1}^m \left| \frac{\partial \omega(\mathbf{a}_0, U)}{\partial a_i} \right| \Delta a_i \quad (21)$$

Similarly, the lower-bound curve and upper-bound curve of transient decay rate coefficient  $\Delta$  varying with  $U$  are, respectively,

$$\underline{\Delta}(\mathbf{a}, U) = \Delta(\mathbf{a}_0, U) - \sum_{i=1}^m \left| \frac{\partial \Delta(\mathbf{a}_0, U)}{\partial a_i} \right| \Delta a_i \quad (22)$$

and

$$\bar{\Delta}(\mathbf{a}, U) = \Delta(\mathbf{a}_0, U) + \sum_{i=1}^m \left| \frac{\partial \Delta(\mathbf{a}_0, U)}{\partial a_i} \right| \Delta a_i \quad (23)$$

The freestream velocity corresponding to the null of Eq. (22) is the upper bound  $\bar{U}_{\text{cr}}$  of flutter speed  $U_{\text{cr}}$ , and the freestream velocity corresponding to the null of Eq. (23) is the lower bound  $\underline{U}_{\text{cr}}$  of flutter speed  $U_{\text{cr}}$ . Thus, the approximate estimation of flutter speed interval is

$$U_{\text{cr}}^I = [\underline{U}_{\text{cr}}, \bar{U}_{\text{cr}}] \quad (24)$$

The middle values  $\omega(\mathbf{a}_0, U)$  and  $\Delta(\mathbf{a}_0, U)$  in Eqs. (16–23) can be obtained by the PK method, solving Eq. (10) under the conditions of the given nominal value  $\mathbf{a}_0$  of uncertain parameter and the velocity  $U$ . For the computation of the partial derivatives  $\partial \omega(\mathbf{a}_0, U)/\partial a_i$  and  $\partial \Delta(\mathbf{a}_0, U)/\partial a_i$ , due to the complicated implicit function relationship between  $\omega$  and  $\Delta$ , it is not easy to obtain their analytical expression. One practical method is to adopt the difference approximation.

#### IV. Nonprobabilistic Interval Reliability of Wing Flutter

##### A. Flutter-Wind-Speed and Natural-Wind-Speed Interference Model for Flutter Reliability

In this section, the flutter reliability of the wing will be assessed based on the general nonprobabilistic interval reliability model [15], in which the compatibility between the nonprobability interval safety measure and the probabilistic reliability has been demonstrated. The limit state of flutter is expressed as the function of flutter wind speed  $U_{\text{cr}}$  and natural wind speed  $U_b$  as follows:

$$M = M(U_{\text{cr}}, U_b) = U_{\text{cr}} - U_b = 0 \quad (25)$$

Because of the influences of the uncertain factors in wing structure and natural wind flow,  $U_{\text{cr}}$  and  $U_b$  will be uncertain. Based on the assumption of nonprobabilistic interval reliability model,  $U_{\text{cr}}$  and  $U_b$  will vary within the certain ranges: that is,

$$\underline{U}_{\text{cr}} \leq U_{\text{cr}} \leq \bar{U}_{\text{cr}}, \quad \underline{U}_b \leq U_b \leq \bar{U}_b \quad (26)$$

where  $\underline{U}_{\text{cr}}$  and  $\bar{U}_{\text{cr}}$  are, respectively, the lower bound and upper bound of flutter speed, and  $\underline{U}_b$  and  $\bar{U}_b$  are, respectively, the lower bound and upper bound of natural wind speed.

By the use of the interval notations in interval mathematics [12,13], the inequalities (26) can be rewritten as

$$U_b \in [\underline{U}_b, \bar{U}_b], \quad U_b \in [\underline{U}_b, \bar{U}_b] \quad (27)$$

Then the flutter-speed interval and natural-wind-speed interval can be expressed, respectively, as

$$U_{\text{cr}}^I = [\underline{U}_{\text{cr}}, \bar{U}_{\text{cr}}] \quad (28)$$

$$U_b^I = [\underline{U}_b, \bar{U}_b] \quad (29)$$

where  $U_{\text{cr}}^I$  can be obtained by the previous interval finite element analysis of flutter, and  $U_b^I$  can be obtained by the practical measurements.

The flutter wind speed and natural wind speed have the same physical dimensions. Thus, their interval descriptions can be placed on a number axis. During the design process of the wing, the flutter speed is required to be larger than the actual wind speed, implying that the wing with respect to the median values must be safe (i.e.,  $U_{\text{cr}}^c > U_b^c$ ). But due to the scatter in  $U_{\text{cr}}$  and  $U_b$ , the intervals themselves may share the same numerical values to yield an intersection set, as shown in Fig. 1 as the shaded region. This region can be called the interference region. Similar to the terminology in probabilistic reliability theory, Fig. 1 can be dubbed as the nonprobabilistic interval flutter-wind-speed and natural-wind-speed interference model. We are interested in adopting a measure of safety

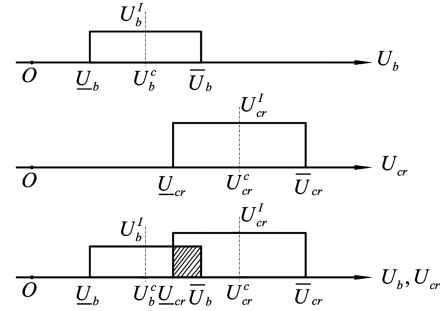


Fig. 1 Flutter speed and wind speed interference model for flutter reliability.

that is interconnected with the lower and upper bounds of flutter wind speed and natural wind speed.

##### B. Measure of Nonprobabilistic Interval Reliability of Flutter

When the interference between the flutter-wind-speed interval and natural-wind-speed interval occurs, as shown Fig. 2, though the median value  $U_b^c$  of the natural wind speed is smaller than the median value  $U_{\text{cr}}^c$  of the flutter wind speed, it cannot be ensured that the natural wind speed will take on values not in excess of the flutter wind speed. Thus, the possibility that the natural wind speed is larger than the flutter wind speed will be different from zero. This fact can be expressed as

$$\eta(M(U_{\text{cr}}, U_b) < 0) > 0 \quad (30)$$

where  $\eta(T)$  represents the possibility of the event  $T$ .

It is instructive to represent the flutter wind speed and natural wind speed in a plane, as shown in Fig. 2. The solid rectangle shows the region of variation of both  $U_{\text{cr}}$  and  $U_b$ . It is being crossed by the failure plane  $U_{\text{cr}} = U_b$ . The safe region is again hatched, whereas the failure region is unshaded. The possibility that Eq. (30) holds or the possibility that the natural wind speed is larger than the flutter wind speed will be referred to as the nonprobabilistic interval failure measure, which can be defined as the ratio of the area of failure region to the total area of basic variables region: that is,

$$F_{\text{flutter}} = \eta(M(R, S) < 0) = \frac{A_{\text{failure}}}{A_{\text{total}}} \quad (31)$$

The possibility that the natural wind speed is smaller than the flutter wind speed is defined herewith as the nonprobabilistic interval safety measure. It can be defined as the ratio of the area of the safe region to the total area of basic variables region: that is,

$$S_{\text{flutter}} = \eta(M(R, S) > 0) = \frac{A_{\text{safe}}}{A_{\text{total}}} \quad (32)$$

It is seen that it is easier to evaluate  $A_{\text{failure}}$  than  $A_{\text{safe}}$ . Therefore, we represent  $S_{\text{flutter}}$  as its complement to  $F_{\text{flutter}}$ : that is,

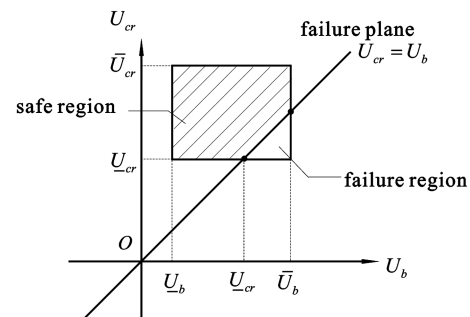


Fig. 2 Scheme I for the space of variables under interference occurrence.

$$S_{\text{flutter}} = 1 - F_{\text{flutter}} = 1 - \frac{A_{\text{failure}}}{A_{\text{total}}} \quad (33)$$

When the interference between the natural wind speed and the flutter wind speed does not take place or when the maximum value or upper bound of the natural wind speed is equal to or smaller than the minimum value or lower bound of the flutter wind speed, the event in which the natural wind speed is bigger than the flutter wind speed is impossible. In other words, the possibility that the natural wind speed is bigger than the flutter wind speed is zero: that is,

$$F_{\text{flutter}} = \eta(M(R, S) > 0) = \frac{A_{\text{failure}}}{A_{\text{total}}} = 0 \quad (34)$$

The state when the upper bound  $\bar{U}_b$  of the natural wind speed is equal to the lower bound  $\underline{U}_{\text{cr}}$  of the flutter wind speed could be called the *critical state*, as shown in Fig. 3.

The value of the possibility of failure strongly depends on the middle and radius values of interval variables  $\underline{U}_b^l$  and  $\bar{U}_{\text{cr}}^l$ . When the rectangle is mostly above the limit state,  $A_{\text{failure}}$  can be calculated easily according to the geometric relation in Figs. 2 and 3.  $A_{\text{failure}}$  is equal to the area of triangle for the failure region: namely,  $A_{\text{failure}} = \frac{1}{2}(\bar{U}_b - \underline{U}_{\text{cr}})^2$ . Particularly when the rectangle is completely above the limit state, it is obvious that  $A_{\text{failure}} = 0$ . Otherwise, as shown in Figs. 4–6, the calculations of  $A_{\text{failure}}$  are relatively complex. Nevertheless, in practice, the scheme design for the wing usually requires a lower possibility of failure, as shown in Fig. 2.

## V. Numerical Examples

In this section, a three-degree-of-freedom airfoil and fuselage and a 15-deg swept-back wing are used to illustrate the feasibility of the proposed method for the nonprobabilistic interval reliability of flutter.

### A. Example I: Three-Degree-of-Freedom Airfoil and Fuselage

As shown in Fig. 7, the airfoil is connected to the fuselage mass by bending and torsion springs, and the fuselage is free to plunge. The length of the wing chord is  $2B = 1.8$  m. The airfoil center of gravity is at 37% of the wing chord, its aerodynamic center is at 25% of the

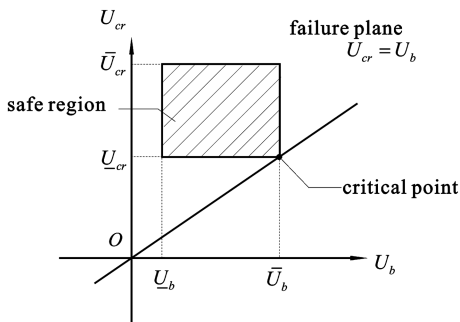


Fig. 3 Representation for the critical state.

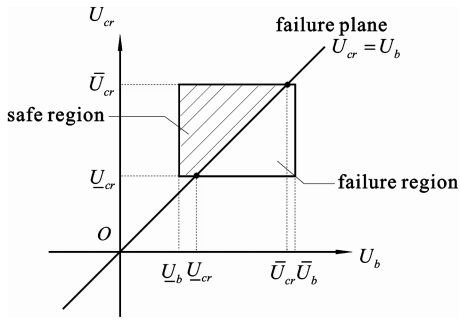


Fig. 4 Scheme II for the space of variables.

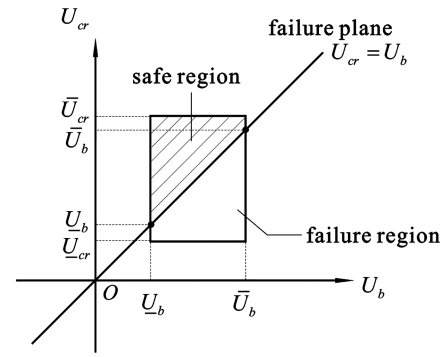


Fig. 5 Scheme III for the space of variables.

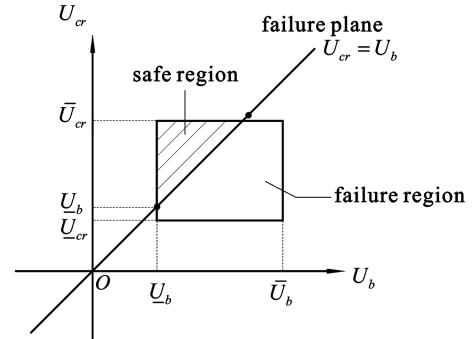


Fig. 6 Scheme IV for the space of variables.

wing chord, and the springs are connected to the elastic axis at 40% of the wing chord. The airfoil lift-curve slope is the theoretical two-dimensional incompressible value of  $c_{la} = 2\pi$ . The fuselage mass is 2000 kg. The bending stiffness and bending damping of the spring are, respectively, 2000.0 N/m and 6 N · s/m, and the torsion stiffness and torsion damping are, respectively, 2000.0 and 3 N · m · s/rad.

Suppose that the airfoil mass and the moment of inertia about the elastic axis are uncertain parameters and their interval numbers are  $m_a^l = [1700, 2300]$  kg and  $I_a^l = [0.9, 1.1] \times 10^{-4}$  kg · m<sup>2</sup>. For comparing with the stochastic finite element model [5], it is also assumed that the two uncertain parameters have the normal distributions within the given intervals. According to the  $3\sigma$  rule, their mean values and standard deviations are  $\mu_{m_a} = 2000$  kg,  $\mu_{I_a} = 1.0 \times 10^{-4}$  m<sup>4</sup>,  $\sigma_{m_a} = 50$  kg, and  $\sigma_{I_a} = 3 \times 10^{-6}$  m<sup>4</sup>. This example uses strip-theory aerodynamics with the W.P. Jones approximation to the Theodorsen circulation function. The lower-bound and upper-bound curves of  $V-g$  ( $g = 2\Delta$ ) obtained by the interval finite element model for uncertain flutter analysis are shown in Fig. 8. Figure 8 also gives the lower-bound and upper-bound

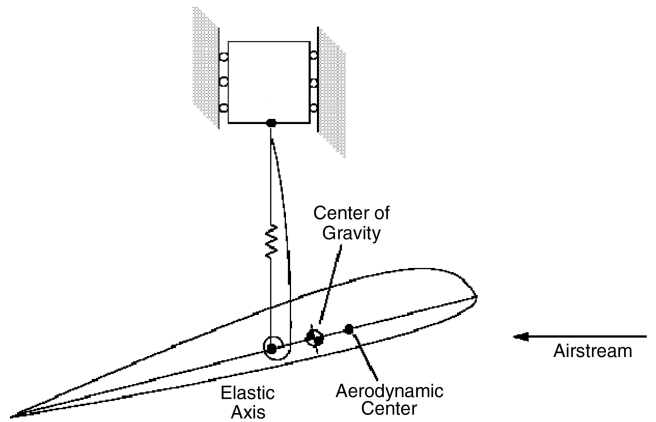


Fig. 7 Three-degree-of-freedom airfoil and fuselage.

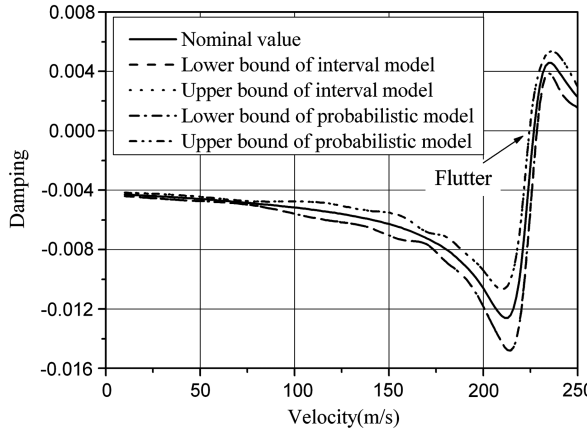


Fig. 8 Lower bound and upper bound of  $V-g$  curves.

curves of  $V-g$  ( $g = 2\Delta$ ) obtained by the stochastic finite element model, which can be obtained by the probabilistic region of 3 times the standard deviation of its mean value of  $g$ . It can be seen from Fig. 8 that the lower-bound and upper-bound curves obtained by the interval finite element model are in good agreement with those obtained by the stochastic finite element model. So the interval estimation of flutter speed obtained by both of the two models is  $U_{cr}^l = [224.70, 228.72]$  m/s.

Because of the uncertainty of natural wind speed in practice, it cannot usually be exactly measured, but a range containing the exact value can be known. Here, it is assumed that the interval of the natural wind speed can be obtained as  $U_b^l = [222.0, 225.0]$  m/s by the measurement. By the use of Eq. (33), the nonprobabilistic flutter safety measure can be obtained as follows:

$$\begin{aligned} S_{\text{flutter}} &= \frac{A_{\text{safe}}}{A_{\text{total}}} = 1 - \frac{A_{\text{failure}}}{A_{\text{total}}} \\ &= 1 - \frac{1/2(\bar{U}_b - \underline{U}_{cr})^2}{(\bar{U}_b - \underline{U}_b)(\bar{U}_{cr} - \underline{U}_{cr})} = 1 - \frac{1/2(\bar{U}_b - \underline{U}_{cr})^2}{2U_b^r \cdot 2U_{cr}^r} \\ &= 1 - \frac{(\bar{U}_b - \underline{U}_{cr})^2}{8U_b^r U_{cr}^r} = 99.63\% \end{aligned}$$

where  $r$  stands for the uncertain radius of the interval variable.

Similar to the probabilistic reliability, the nonprobabilistic interval reliability represents the possibility that the designed wing will perform a required function under stated conditions for a stated period of time. The larger the  $S_{\text{flutter}}$  values, the higher the reliability of the wing flutter. Reliability analysis is performed for the assessment of reliability to the designed structure. If the calculated reliability for the designed wing is larger than the prespecified reliability level, then it will be considered as an acceptable design; otherwise, it is an exceptional design.

#### B. Example II: 15-Degree Swept-Back Wing

A 15-deg swept-back wing, as shown in Fig. 9, is considered. The length of the wing chord is  $2B = 2.076$  m and the length of the wing span is  $l = 5.72$  m. The airfoil consists of several independent segments, including the beveled leading- and trailing-edge regions with constant thickness in between. The airfoil thickness is 0.041 m, and it is beveled between the first and last one-eighth of the wing chord. The material of this wing is aluminum alloy, and its Poisson ratio is  $\nu = 0.3$ .

Because of the scattering of material property, its elastic modulus and density are uncertain and their intervals are  $E^l = [67.0, 73.0] \times 10^9$  N/m<sup>2</sup> and  $\rho^l = [2600.0, 2800.0]$  kg/m<sup>3</sup>. For comparing with the stochastic finite element model, it is also assumed that the elastic modulus and density are normal or Gaussian distributions in their interval numbers, with the mean values of  $\mu_E = 70.0 \times 10^9$  N/m<sup>2</sup> and  $\mu_\rho = 2700.0$  kg/m<sup>3</sup> and the standard deviations of  $\sigma_{ma} = 1.0 \times 10^9$  N/m<sup>2</sup> and  $\sigma_\rho = 33.3$  kg/m<sup>3</sup>. This example adopts piston-

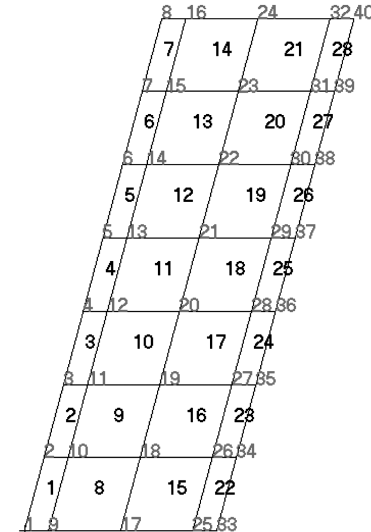


Fig. 9 Fifteen-degree swept-back wing.

theory aerodynamics with the Van Dyke correction. The lower-bound and upper-bound curves of  $V-g$  ( $g = 2\Delta$ ) obtained by the proposed interval finite element model for uncertain flutter analysis are shown in Fig. 10. Figure 10 also gives the lower-bound and upper-bound curves of  $V-g$  ( $g = 2\Delta$ ) obtained by the stochastic finite element model, which can be obtained by the probabilistic region of 3 times the standard deviation of its mean value of  $g$ .

It can be seen from Fig. 10 that the interval of damping  $g$  obtained by the interval finite element model is slightly wider than that obtained by the stochastic finite element model. Namely, the upper bound of damping  $g$  obtained by the proposed model is slightly larger than that obtained by the stochastic finite element model, and the lower bound of damping  $g$  obtained by the proposed model is slightly smaller than that obtained by the stochastic finite element model. The interval estimation of flutter speed obtained from the upper-bound and lower-bound curves of the proposed interval finite element model is  $U_{cr}^l = [759.00, 776.83]$  m/s, and the flutter speed obtained from the upper-bound and lower-bound curves of the proposed stochastic finite element model is  $U_{cr}^r = [759.03, 776.67]$  m/s. Therefore, in case the known information on uncertainties is too scant to determine their statistical characteristics, the proposed interval finite element model can give a better estimation of the flutter speed of the wing with uncertainties.

The interval estimation of flutter speed obtained from the upper-bound and lower-bound curves of the interval finite element model is  $U_{cr}^l = [759.00, 776.83]$  m/s. In this example, it is assumed that the interval of the natural wind speed can be obtained as  $U_b^l = [750.0, 765.0]$  m/s by the measurement. By the use of Eq. (33), the nonprobabilistic flutter safety measure can be obtained as follows:

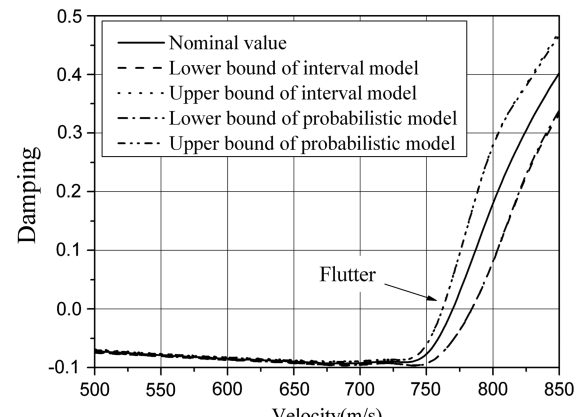


Fig. 10 Lower bound and upper bound of  $V-g$  curves.

$$S_{\text{flutter}} = \frac{A_{\text{safety}}}{A_{\text{total}}} = 1 - \frac{A_{\text{failure}}}{A_{\text{total}}} = 1 - \frac{(\bar{U}_b - U_{\text{cr}})^2}{8U_b^r U_{\text{cr}}^r} = 93.27\%$$

## VI. Conclusions

In this paper, a new measure of flutter reliability of the wing is proposed when analyzing uncertainty in a nonprobabilistic manner. The reliability measure is defined as the ratio of the volume of the safe region to the whole volume of variation of uncertain variables. It has a simple geometric meaning, in addition to being a nondimensional quantity.

The prominent advantage of the proposed model is that only the bounds of uncertain parameters are required, and the probabilistic distribution densities or other statistical characteristics are not needed. In the absence of enough information on uncertainty in structural parameters of the wing and natural wind, the presented nonprobabilistic interval reliability theory may give an alternative assessment of flutter safety.

## Acknowledgments

X. Wang and Z. Qiu thank the National Outstanding Youth Science Foundation of the People's Republic of China (no. 10425208), 111 Project (no. B07009), and FanZhou Science and Research Foundation for Young Scholars (no. 20080503) for support.

## References

- [1] Dowell, E. H., *A Modern Course in Aeroelasticity*, Kluwer Academic, Boston, 2004.
- [2] Ueda, T., "Aeroelastic Analysis Considering Structural Uncertainty," *Aviation*, Vol. 9, No. 1, 2005, pp. 3–7.
- [3] Ito, M., and Fujino, Y., "A Probabilistic Study of Torsional Flutter of Suspension Bridge Under Fluctuating Wind," *Proceedings of the Fourth International Conference on Structural Safety and Reliability*, American Society of Civil Engineers, New York, 1985, pp. 145–160.
- [4] Ostenfeld-Rosenthal, P., Madsen, H. O., and Larsen, A., "Probabilistic Flutter Criteria for Long Span Bridges," *Journal of Wind Engineering and Industrial Aerodynamics*, Vol. 42, Nos. 1–3, 1992, pp. 1265–1276. doi:10.1016/0167-6105(92)90133-U
- [5] Ge, Y. J., and Xiang, H. F., "Stochastic Finite Element Analysis of Bridge Flutter," *China Civil Engineering Journal*, Vol. 32, No. 4, 1999, pp. 27–32 (in Chinese).
- [6] Ge, Y. J., and Xiang, H. F., "Reliability Analysis of Bridge Flutter Under Stochastic Wind Loading," *China Civil Engineering Journal*, Vol. 36, No. 6, 2003, pp. 42–46.
- [7] Ge, Y. J., Zhou, Z., and Xiang, H. F., "Reliability Assessment of Bridge Flutter Based on Modified FOSM Method," *Structural Engineers*, Vol. 22, No. 3, 2006, pp. 46–51 (in Chinese).
- [8] Liu, Y. W., Chen, Q. L., and Zheng, D. Q., "Flutter Reliability Analysis of Wing Structure," *Chinese Journal of Aeronautics*, Vol. 19, No. 4, 1997, pp. 503–505 (in Chinese).
- [9] Zhu, L. P., Elishakoff, I., and Starnes, J. H., Jr., "Derivation of Multi-Dimensional Ellipsoidal Convex Model for Experimental Data," *Mathematical and Computer Modelling*, Vol. 24, No. 2, 1996, pp. 103–114. doi:10.1016/0895-7177(96)00094-5
- [10] Zuccaro, G., Elishakoff, I., and Baratta, A., "Antioptimization of Earthquake Excitation and Response," *Mathematical Problems in Engineering*, Vol. 4, No. 1, 1998, pp. 1–19. doi:10.1155/S1024123X98000696
- [11] Ben-Haim, Y., and Elishakoff, I., *Convex Models of Uncertainty in Applied Mechanics*, Elsevier Science, Amsterdam, 1990.
- [12] Moore, R. E., *Methods and Applications of Interval Analysis*, Prentice-Hall, London, 1979.
- [13] Alefeld, G., and Herzberger, J., *Introduction to Interval Computations*, Academic Press, New York, 1983.
- [14] Qiu, Z. P., *Convex Method Based on Non-Probabilistic Set Theory and Its Applications*, National Defence Industry Press, Beijing, 2005 (in Chinese).
- [15] Wang, X. J., Qiu, Z. P., and Elishakoff, I., "Non-Probabilistic Set-Theoretic Model for Structural Safety Measure," *Acta Mechanica*, Vol. 198, Nos. 1–2, 2008, pp. 51–64. doi:10.1007/s00707-007-0518-9

A. Messac  
Associate Editor